SUPPLEMENTARY INFORMATION

Tailored graft-type polymer for dopant-free hole transport material in indoor perovskite photovoltaics

Henry Opoku,[a†] Yun Hoo Kim,[b†] Ji Hyeon Lee,[a†] Hyungju Ahn,[c] Jae-Joon Lee,[a] Se-Woong Baek[b]* and Jea Woong Jo [b]*

[a] Department of Energy and Materials Engineering and Research Center for Photoenergy Harvesting & Conversion Technology (phct), Dongguk University, 30 Pildong-ro, 1-gil, Jung-gu, Seoul 04620, Republic of Korea. *E-mail: whwp78@gmail.com (J.W. Jo).

[b] Department of Chemical and Biological Engineering, Korea University, Seoul 02481, Republic of Korea. *E-mail: sewoongbaek@korea.ac.kr (S.-W. B.).

[c] Pohang Accelerator Laboratory, Kyungbuk, Pohang 37673, Republic of Korea.

† H.O., Y.H.K., and J.H.L. contributed equally to this work.

Keywords: graft-type semiconducting conjugated polymers, surface passivation, chemical structure tuning, perovskite photovoltaics, indoor light recycling, dopant-free hole-transporting materials

Experimental section

Materials. 2,6-Bis(trimethytin)-4,8-bis(5-(2-ethylhexyl)thiophen-2-yl)benzo[1,2-b:4,5-b′]dithiophene monomer (**1**) was purchased from SunaTech Inc., and thiophene-terminated PEG (M_n ~ 2.0 KDa) monomer (**3**) was prepared by following previous method.[S1] PbI_2 and $PbBr_2$ were obtained from Tokyo Chemical Industry. Methylammonium iodide and formamidinium iodide were purchased from Great Cell Solar. All unspecified chemicals were purchased from Sigma-Aldrich.

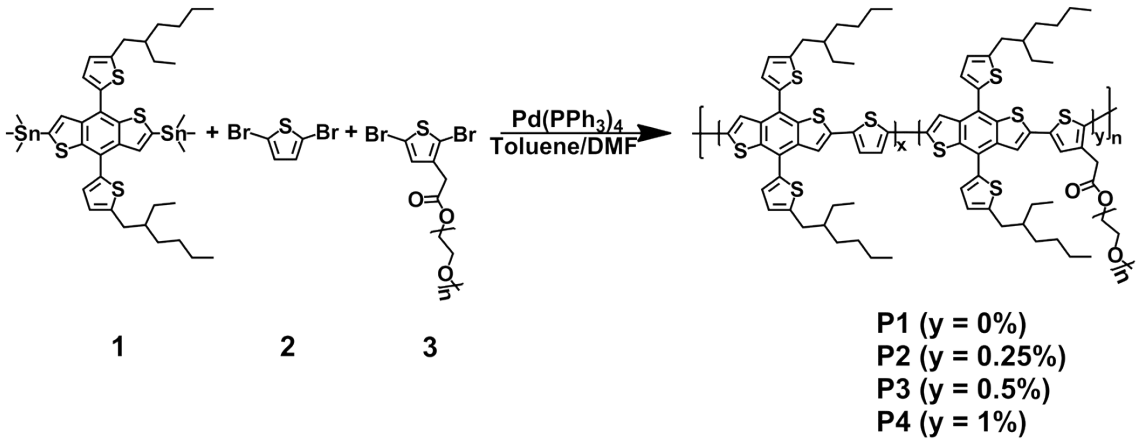

Scheme S1 Synthesis of homopolymer P1 and PEG-grafted copolymers P2, P3 and P4 (M_n of PEG ~ 2 KDa).

Polymerization. For control polymer P1, **1** (400 mg, 0.442 mmol), **2** (107 mg, 0.442 mmol), and $Pd(PPh_3)_4$ (10 mg) were dissolved in a 10 mL of toluene/dimethylformamide (DMF) solvent (5:1 v/v). Polymerization was carried out at 110 °C for 48 h under N_2 protection and the mixture was subsequently cooled to room temperature. The polymer precipitate was then obtained by pouring in methanol and was collected by filtering into Soxhlet thimble. The oligomers and catalyst residues within the synthesized polymer were removed by Soxhlet extraction with

methanol, acetone, ethyl acetate, and hexane. Finally, a dark reddish polymer P1 was obtained by extraction with chloroform and precipitation in methanol (68% yield). PEG-grafted copolymers P2, P3, and P4 were synthesized following the same procedure as P1. For P2, **1** (400 mg, 0.442 mmol), **2** (106.7 mg, 0.441 mmol), and **3** (2.5 mg, 0.0011 mmol) were used and gave a dark red colored material (62% yield). P3 was also synthesized using **1** (400 mg, 0.442 mmol), **2** (106.4 mg, 0.440 mmol), and **3** (5.1 mg, 0.0022 mmol) (65% yield). P4 was also synthesized using **1** (400 mg, 0.442 mmol), **2** (105.9 mg, 0.438 mmol), and **3** (10.2 mg, 0.0044 mmol) (68% yield). Synthesized polymers showed good solubility in chloroform and chlorobenzene solvents with a maximum solubility ~ 35 mg ml^{-1}

Table S1 Molecular weight characteristic of synthesized polymers

HTM	M_n [kDa]	PDI
P1	12.9	1.18
P2	13.1	1.22
P3	13.3	1.32
P4	14.3	1.21

Polymer Characterization. UV–Vis spectra analysis was performed using a Lambda 20 (Perkin Elmer) diode array spectrophotometer. The chemical structures of polymers were investigated by ^1H NMR (Avance DPX-500) using *d*-chloroform ($CDCl_3$) as solvent and tetramethylsilane as internal reference. The molecular weights and polymers distribution were measured by GPC with a refractive index detector (Waters), where tetrahydrofuran solvents were used and polystyrene polymers set as eluent and standards, respectively. Cyclic voltammetry

investigations were carried out with (AutoLab with Weis-500 work station) using a standard three-electrode cell (Ag in 0.1 M $AgNO_3$ reference electrode, Pt wire counter electrode, and Pt working electrode) in 0.1 M tetrabutylammonium hexafluorophosphate in acetonitrile. Thermogravimetric analysis (heating rate = 20 ℃ min^{-1}, N_2 atmosphere) was carried out using TGA N-1000 (Scinco). Surface morphologies of polymer films were investigated *via* tapping-mode atomic force microscopy (AFM) (Nanoscope III, Veeco). GIXRD were carried out at PLS-II 9A U-SAXS beamline of the Pohang Accelerator Laboratory in Korea. SCLC mobilities were estimated using Mott Gurney equation SCLC equation, $J = (9/8)\ \varepsilon_0\ \varepsilon_r\ \mu\ (V^2 / L^3)$, where ε_0 is the permittivity of free space, ε_r is the dielectric constant of active materials, μ is the SCLC mobility, V is the effective applied voltage, and L is the thickness of the polymer film. The configuration of ITO / PEDOT:PSS / polymer / Au was used for fabricating SCLC hole-only devices. Steady-state PL measurements were carried out with cary eclipse fluorescence spectrophotometer (Varian). TR-PL measurements were recorded using a single photon counting system coupled with a single photon counting detector (wavelength of laser source for excitation = 435 nm) (FlouTime 300, PicoQuant).

IPPV fabrication and characterization. ITO / SnO_2 (~20 nm)/ $(MA_{0.91}FA_{0.09})Pb(I_{0.94}Br_{0.06})$ perovskite (~500 nm) / polymer (~90 nm)/ Au (100 nm) configuration was used for IPPVs. Cleaned ITO substrate was UV-treated for 20 m. SnO_2 colloidal solution (15% in H_2O, Alfa Aesar) diluted with 10 mM NaOH solution (1:4 v/v) was spin-casted twice at 4000 rpm for 30 s and annealed at 150 ˚C for 15 m. Perovskite solution was prepared by mixing 200 μL of $MAPbI_3$ solution and 20 μL of $FAPbIBr_2$ solution. $MAPbI_3$ solution was prepared by dissolving PbI_2 (460 mg), methylammonium iodide (159 mg), DMF (630 μL) and dimethyl sulfoxide (67 μL). $FAPbIBr_2$ precursor solution was prepared by dissolving $PbBr_2$ (367 mg), formamidinium iodide (172 mg), dimethyl sulfoxide (78 mg), and DMF (600 mg). The perovskite solution was deposited

by spin-coating on the SnO_2 coated substrate at 1000 rpm for 10 s and at 3500 rpm for 25 s. During the second spin-coating step, 50 μL of chlorobenzene anti-solvent was dropped on the films. Afterwards, the films were annealed at 100 ^oC for 10 m to form perovskite layer. 20 mg mL^{-1} of polymer solutions in chlorobenzene was spin-casted at 2000 rpm for 30 s. Devices were completed by evaporating a 100 nm gold electrode by thermal evaporation through a shadow mask. The device area was 0.2 cm^2. Photovoltaic characteristics of IPPVs were assessed by employing LED lamp (5000 K daylight) (McScience) with the stimulated light calibrated with a standard mono-Si PV device (PVM-396, PV Measurements Inc.) certified by the National Renewable Energy Laboratory. Light intensity was controlled *via* a variable voltage transformers (Hwaseong) and was set at 1000 lux with an irradiance of 0.37 mW cm^{-2} for the investigations of indoor light harvesting. The incident photon to current efficiency (IPCE) of the perovskite devices was estimated with a photo modulation spectroscopy setup (McScience, K3100 Spectral IPCE Measurement System). The power density of the monochromatic light from a xenon lamp was calibrated using a Si photodiode certified by the National Institute for Standards and Technology. Hole-only perovskite devices were also fabricated using a configuration of ITO / PEDOT:PSS / perovskite / HTM / Au. Trap density was estimated from the trap-filled limit voltage (V_{TFL}) region of the resulting curve under dark current according to the equation: $V_{TFL} = e\, n_t\, L^2 / 2\, \varepsilon_r\, \varepsilon_0$, Where L is the thickness of active layer, e is the elementary charge, ε_r is the relative dielectric constant of the perovskite layer, ε_0 is the vacuum permittivity, n_t is the defect density. EIS of devices were measured in the dark with an Autolab PGstat12 potentiostat with an impedance module operating at an applied potential of 0.7 V. One-dimensional perovskite photovoltaics were simulated using the SCAPS-1D software with the configuration of ITO / SnO_2 / perovskite / HTM / Au. The

parameters used for simulation were obtained from literatures and experimental measurements (Table S2).[S2–S5]

Table S2 Parameters used for SCAPS-1D simulation[a]

Parameters	HTM	IL1	Perovskite	IL2	ETM
Thickness [nm]	90	10	500	10	20
Bandgap [eV]	1.95	1.58	1.58	1.58	3.5
EA [eV]	3.18	3.8	3.8	3.8	4
ϵ_r	3.5	6.5	6.5	6.5	9
N_A [cm^{-3}]	$1*10^{17}$	0	0	0	0
N_D [cm^{-3}]	0	10^{15}	10^{16}	10^{15}	10^{14}
μ_e [$cm^2 V^{-1} s^{-1}$]	10^{-4}	2	2	2	20
μ_h [$cm^2 V^{-1} s^{-1}$]	$3.97*10^{-4}$	2	2	2	10
N_t [cm^{-3}]	10^{17}	$4.51*10^{17}$	$5*10^{13}$	10^{13}	10^{15}

[a] ETM: electron transport material; EA: electron Affinity; ϵ_r : permittivity; N_A : acceptor density; N_D: donor density; μ_e : electron mobility; μ_h : hole mobility; N_t : defect density. IL1: HTM/ Perovskite interface layer, IL2: Perovskite/ETM interface layer.

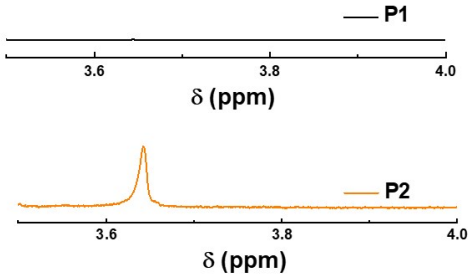

Fig. S1 Magnified ^{1}H-NMR Spectra of P1and P2 polymer indicating PEG proton peak.

Table S3 Comparison of feed ratio and composition of non-grafted thiophene and PEG-grafted thiophene of copolymer.

HTM	Feed ratio of monomers (x unit / y unit)[a]	Composition in copolymer[b] (x unit / y unit)[a]
P2	399	352
P3	199	179
P4	99	91

[a] Scheme S1. [b] Obtained from ^{1}H NMR spectra.

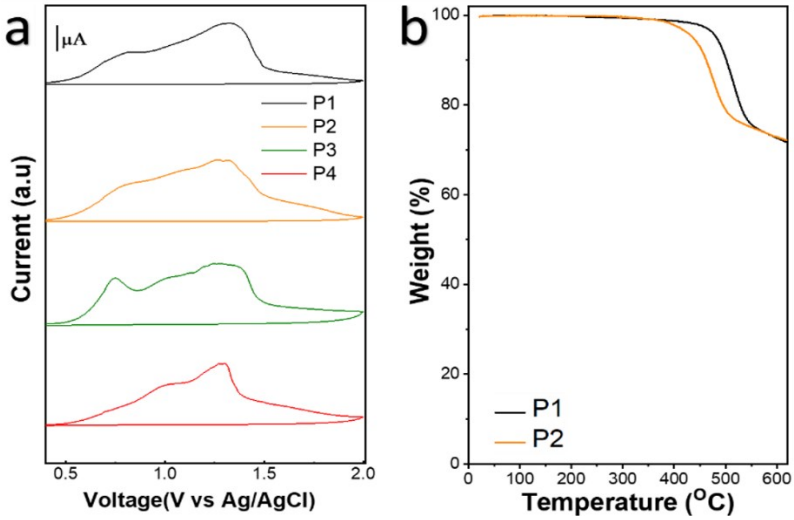

Fig S2. (a) Cyclic voltammetry (CV) of polymers. (b) Thermogravimetric analysis of P1 and P2 polymers.

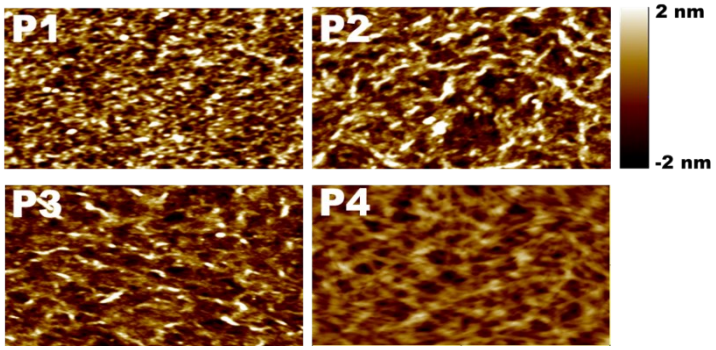

Fig. S3 AFM Topographic images (1 μm × 2 μm) of polymeric HTM films on glass substrate.

Table S4 Fit parameters obtained from TR-PL spectra (Fig. 2c) using a double exponential function ($A_1\exp(-t/t_1) + A_2\exp(-t/t_2)$).

HTM	A_1 [%]	t_1 [ns]	A_2[%]	t_2 [ns]	Average decay time[a] [ns]
P1	21.0	5.10	79.0	143	114
P2	11.2	6.91	88.8	230	204
P3	17.0	6.80	83.0	218	182
P4	19.1	5.77	80.9	159	130

[a] Calculated by using following equation: average decay time = $A_1 \times t_1 + A_2 \times t_2$.

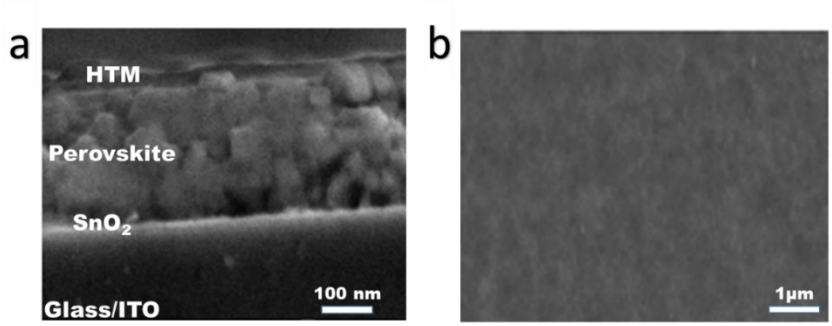

Fig. S4 (a) Cross-sectional SEM image of P2 IPPV. (b) top-surface SEM image of P2 HTM - capped perovskite film.

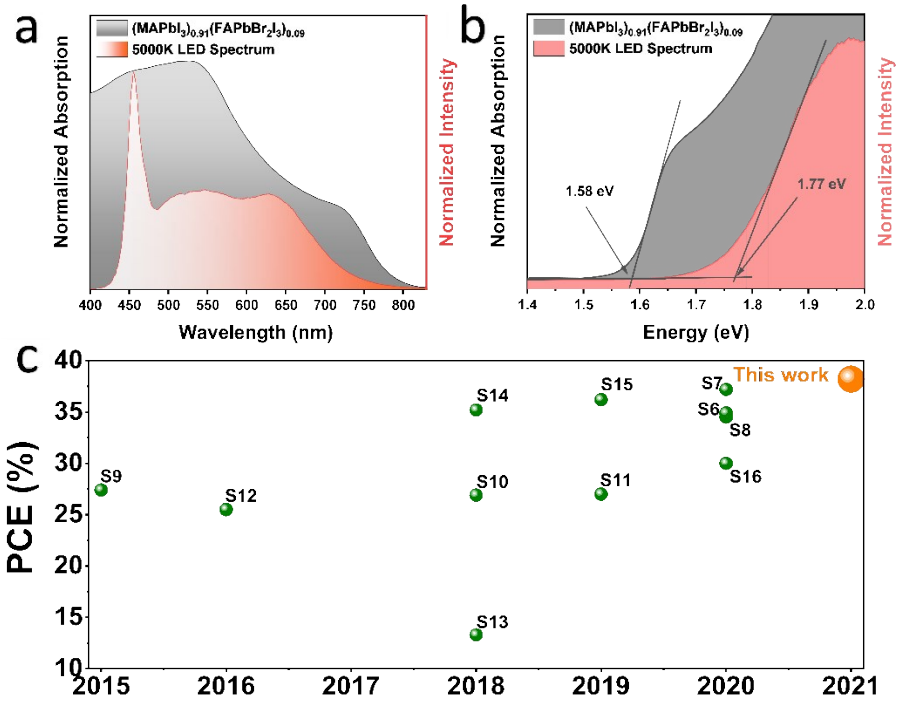

Fig. S5 (a) LED light source and perovskite absorption spectra employed in the study. (b) Optical bandgap (band edge) of perovskite active layer and LED light source used in the study. (c) Comparison of reported PCEs for IPPVs (Table S5).

Table S5 Comparison of reported photovoltaic performances of IPPVs.

HTM[a]	Perovskite (bandgap)	Light source (Intensity)	J_{SC} [μA cm^{-2}]	V_{OC} [V]	FF [%]	PCE [%]	Ref
	Doped HTM[b]						
Spiro-OMeTD	$MAPbI_3$ (1.59 eV)	fluorescent lamp (1000 lux)	175	0.93	60.0	34.9	S6
Spiro-OMeTAD	$MAPbI_3$ (1.55 eV)	LED 6500 K (1000 lux)	157.6	0.98	72.0	37.2	S7
Spiro-OMeTAD	$MAPb(I_{1-x}Br)_3$ (1.72 eV)	LED 1000 Lux	171	0.82	68.8	34.5	S8
Spiro-OMeTAD	$MAPbI_{3x}BrCl_x$ (1.60 eV)	LED 6500K (1000 lux)	137.5	0.85	77.0	27.4	S9
Spiro-OMeTAD	$MAPbI_3$ (1.55 eV)	LED (400 lux)	64.5	0.89	72.0	26.9	S10
Spiro-OMeTAD	$MAPbI_3$ (1.55 eV)	LED 6500K (1000 lux)	129.5	0.86	75.0	27	S11
Spiro-OMeTAD	$MAPbI_3$ (1.55 eV)	CFL/400 lux	58	0.77	72	25.5	S12
Spiro-OMeTAD	$MAPbI_3$ (1.55 eV)	White LED / 400 Lux	47.7	0.84	59.0	13.3	S13
	Inorganic HTM[c]						
NiO_X	$MAPbI_3$ (1.55 eV)	LED (1000 Lux)	150	0.87	75	35.2	S14
NiO_X	$MAPb1_{2-X}BrCl_x$ (1.80 eV)	LED (1000 lux)	126	1.03	76	36.2	S15
	Dopant-free HTM[b]						
TPA-BPFN-TPA	$MAPbI_3$ (1.53 eV)	LED (1000 lux)	186	0.79	74.0	30	S16
P2	**$(MA_{0.91}FA_{0.09})Pb(I_{0.094}Br_{0.06})$ (1.58 eV)**	**LED 5000k (1000 lux)**	**188**	**0.96**	**78.7**	**38.2**	**This work**

[a] Spiro-OMeTAD: 2,2',7,7'-tetrakis[*N*,*N*-di(4-methoxyphenyl)amino]-9,9'-spirobifluorene; TPA-BPFN-TPA: triphenylamine-biphenylfumaronitrile-triphenylamine. [b] *n-i-p* device configuration. [c] *p-i-n* device configuration.

Table S6 Photovoltaic properties of PPVs evaluated under standard AM 1.5G illumination

HTM	J_{SC} [mA cm^{-2}]	V_{OC} [V]	FF [%]	PCE (max) [%]
P1	22.3 ± 0.2	1.07 ± 0.04	70.3 ± 1.5	16.8 ± 0.1 (17.4)
P2	22.7 ± 0.4	1.12 ± 0.02	74.8 ± 1.3	19.0 ± 0.3 (21.7)

Table S7 Comparison of photovoltaic performances of *n-i-p* OPPVs with dopant-free HTMs

HTM[a]	Perovskite (bandgap)	J_{SC} [mA cm^{-2}]	V_{OC} [V]	FF [%]	PCE [%]	Ref
PBDTTDF-TH	$MAPbI_3$ (1.55 eV)	22.8	1.11	80	20.3	S17
PBDTT	$Cs_{0.06}FA_{0.78}MA_{0.14}Pb_{0.94}I_{2.4}Br_{0.45}$ (1.56 eV)	23.6	1.12	76.7	20.3	S18
2DP-TDB	$FA_{0.85}MA_{0.15}PbI_3$. (1.53 eV)[b]	24.02	1.16	79.57	22.17	S19
	Interface modification					
PDCBT[c]	$FA_{0.83}MA_{0.17}Pb_{1.1}Br_{0.50}I_{2.80}$ (1.56 eV)	22.7	1.17	80	21.2	S20
P3HT[d]	$(FAPbI_3)_{0.95}/(MAPbBr_3)_{0.05}$ (1.48 eV)	24.9	1.15	81.4	23.3	S21
P3HT[e]	$(FAPbI_3)_{0.95}(MAPbBr_3)_{0.05}$ (1.48 eV)	25.3	1.09	77.4	21.4	S22
P3HT[d,e]	$(FAPbI_3)_{0.95}(MAPbBr_3)_{0.05}$ (1.48 eV)	25.5	1.15	83.8	24.6	S22
	Ethylene glycol-based side chain					
PTEG	$Cs_{0.05}FA_{0.81}MA_{0.14}PbI_{2.55}$ $Br_{0.45}$ (1.56 eV)	22.5	1.14	77	19.8	S23
Alkoxy-PTEG (2-MA)	$Cs_{0.06}FA_{0.78}MA_{0.14}Pb_{0.94}I_{2.4}Br_{0.45}$ (1.56 eV)	23.2	1.14	79.8	21.2	S24
DTB (0.03DEG)	$Cs_{0.05}FA_{0.81}MA_{0.15}/PbI_{2.255}Br_{0.45}$ (1.56 eV)	23.6	1.14	75.1	20.2	S25
P2	**$(MA_{0.91}FA_{0.09})Pb(I_{0.094}Br_{0.06})$** (1.58 eV)	**24.0**	**1.16**	**77.9**	**21.7**	**This Work**

[a] PBDTTDF-TH: 4,8-bis(5-(2-ethylhexyl)-4-fluorothiophene-2-yl)BDT + thiophene-based polymer; PBDTT: indacenodithiophene + benzodithiophene-4,8-dione (BDD)-based polymer; 2DP-TDB: diketopyrrolopyrrole (DPP) + BDT 2D polymer; PDCBT: poly[5,5'-bis(2-butyloctyl)-(2,2'-bithiophene)-4,4'-dicarboxylate-alt-5,5'-2,2'-bithiophene]; P3HT: poly(3-hexylthiophene); PTEG and Alkoxy-PTEG: BDT + 2,1,3-benzothiadiazol-based polymer; DTB(0.03DEG): dithiophene + benzene-based polymer. [b] Component tuning with 4-fluorobenzamide hydrochloride. [c] Ta-WO_x/polymer multilayer. [d] Double halide architecture using *n*-hexyl trimethyl ammonium bromide treatment. [e] $Ga(acac)_3$ additive.

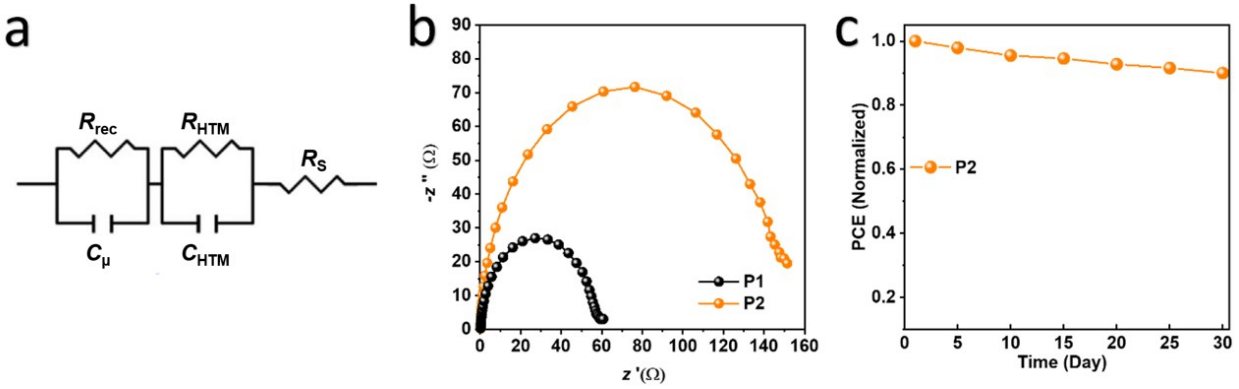

Fig. S6 (a) Equivalent circuit model employed for EIS analysis: electronic parameters includes the series resistance (R_s), HTM capacitance (C_{HTM}), HTM resistance (R_{HTM}), chemical capacitance (C_μ) and the recombination resistance within perovskite (R_{rec}). These were extracted by fitting with the equivalent circuit.[S26] (b) Nyquist plots obtained under dark condition at a biased voltage of 0.7 V for P1 and P2 capped IPPVs. (c) Atmospheric stability test of unencapsulated IPPVs capped with P2 HTM (40% relative humidity and 25 ℃ room temperature).

HTM	R_S [Ω]	Interface recombination lifetime [μs]	Bulk recombination lifetime [μs]
P1	60.5	3.14	135
P2	44.8	187	239

Table S8 EIS fitting parameters for P1 and P2 IPPVs.

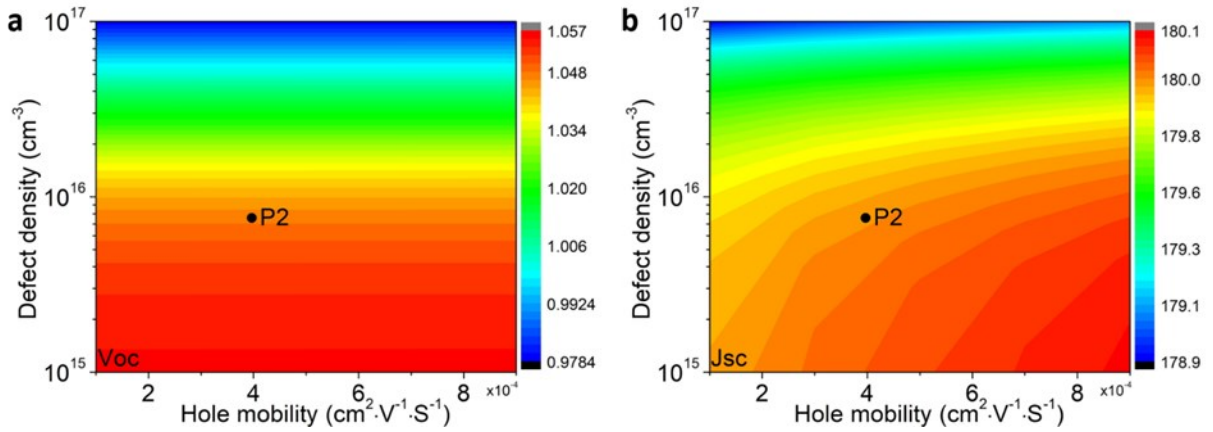

Fig. S7 Calculated (a) V_{OC}, (b) J_{SC} contour plot depending on the hole mobility and defect density under the indoor light illumination.

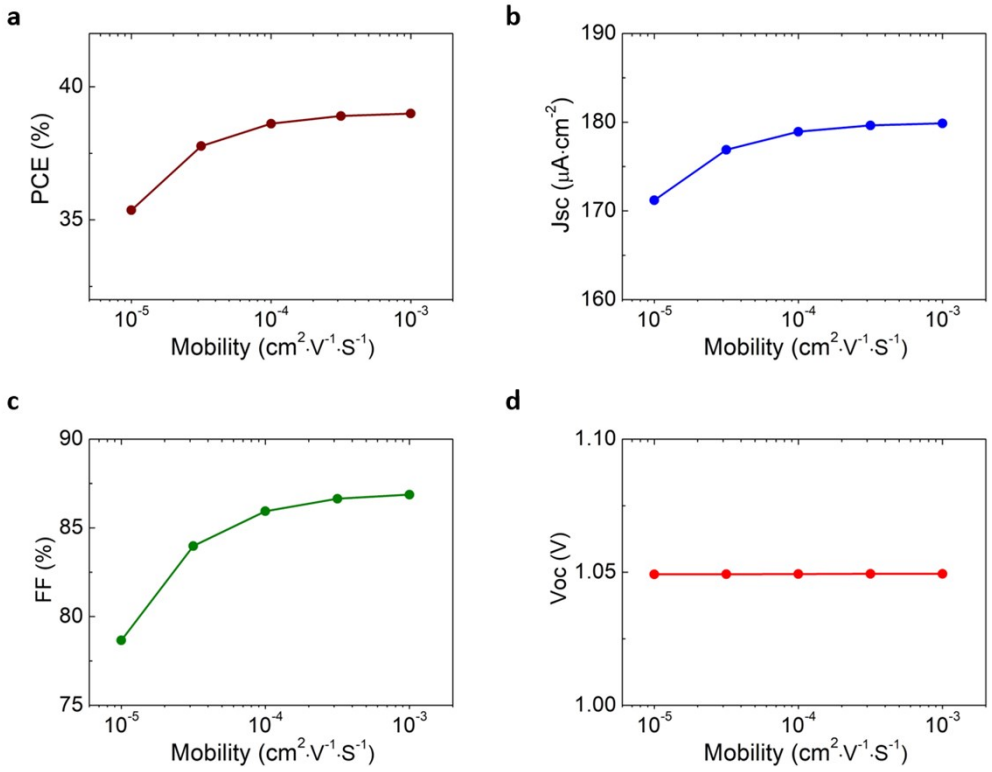

Fig. S8 Calculated perovskite PV parameters depending on the hole mobility of HTM: (a) V_{OC}, (b) J_{SC}, (c) FF, and (d) PCE, respectively.

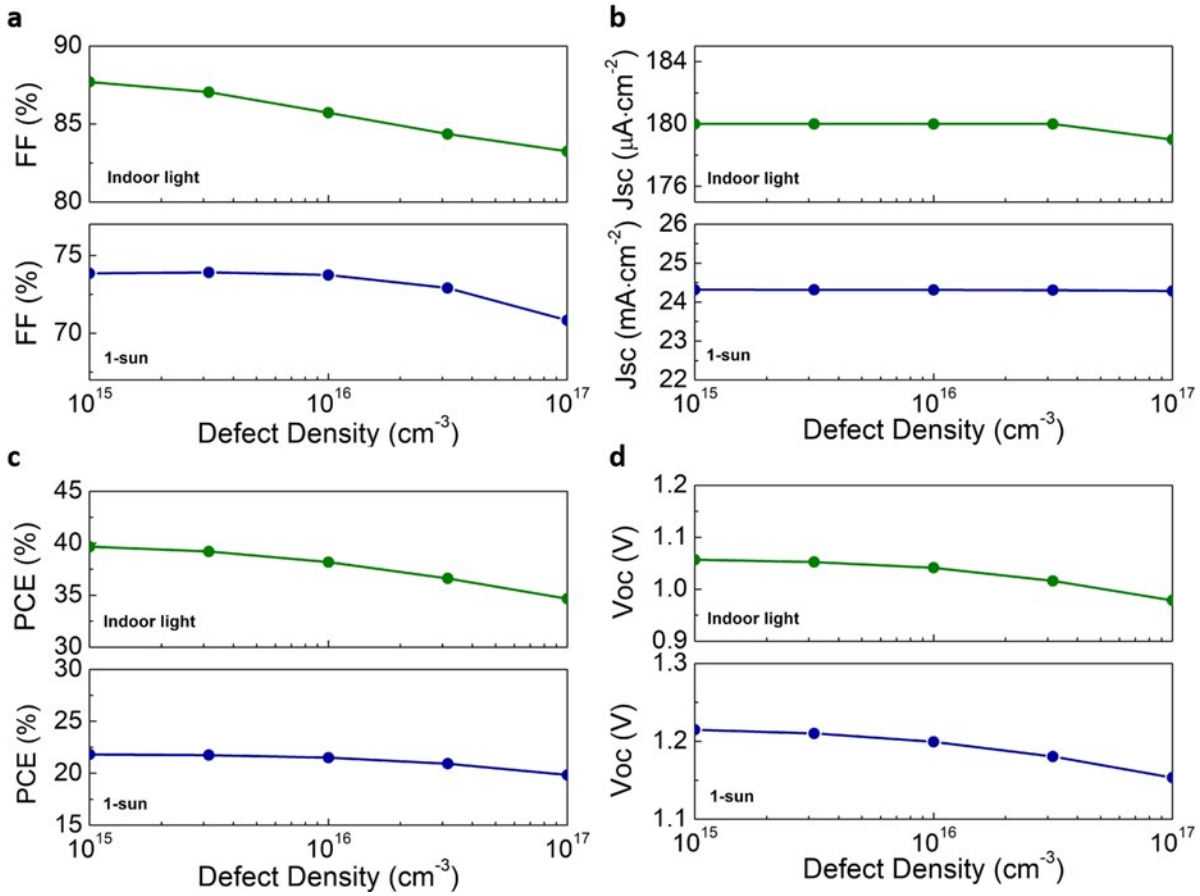

Fig. S9 Calculated perovskite PV parameters: (a) FF, (b) J_{SC}, (c) V_{OC}, and (d) PCE under the indoor light (green) and 1-sun (blue) illuminations, respectively.

References

S1 J. U. Lee, J. Huh, K. H. Kim, C. Park and W. H. Jo, *Carbon*, 2007, **45**, 1051–1057.

S2 S. Karthick, S. Velumani and J. Bouclé, *Solar Energy*, 2020, **205**, 349–357.

S3 A. S. Chouhan, N. P. Jasti and S. Avasthi, *Mater. Lett.*, 2018, **221**, 150–153.

S4 S. Foster, F. Deledalle, A. Mitani, T. Kimura, K. B. Kim, T. Okachi, T. Kirchartz, J. Oguma, K. Miyake, J. R. Durrant, S. Doi and J. Nelson, *Adv. Energy Mater.*, 2014, **4**, 1400311.

S5 Y. Li, W. Yan, Y. Li, S. Wang, W. Wang, Z. Bian, L. Xiao and Q. Gong, *Sci. Rep.*, 2015, **5**, 14485.

S6 C. Dong, M. Li, Y. Zhang, K. L. Wang, S. Yuan, F. Igbari, Y. Yang, X. Gao, Z. K. Wang and L. S. Liao, *ACS Appl. Mater. Interfaces*, 2020, **12**, 836–843.

S7 Y. W. Noh, I. S. Jin, K. S. Kim, S. H. Park and J. W. Jung, *J. Mater. Chem. A*, 2020, **8**, 17163–17173.

S8 J. W. Lim, H. Kwon, S. H. Kim, Y. J. You, J. S. Goo, D. H. Ko, H. J. Lee, D. Kim, I. Chung, T. G. Kim, D. H. Kim and J. W. Shim, *Nano Energy*, 2020, **75**, 104984.

S9 C. Y. Chen, J. H. Chang, K. M. Chiang, H. L. Lin, S. Y. Hsiao and H. W. Lin, *Adv. Funct. Mater.*, 2015, **25**, 7064–7070.

S10 J. Dagar, S. Castro-Hermosa, G. Lucarelli, F. Cacialli and T. M. Brown, *Nano Energy*, 2018, **49**, 290–299.

S11 R. Cheng, C. C. Chung, H. Zhang, Z. Zhou, P. Zhai, Y. T. Huang, H. Lee and S. P. Feng, *Small*, 2019, **15**,1804465 .

S12 F. Di Giacomo, V. Zardetto, G. Lucarelli, L. Cinà, A. Di Carlo, M. Creatore and T. M. Brown, *Nano Energy*, 2016, **30**, 460–469.

S13 J. Dagar, S. Castro-Hermosa, M. Gasbarri, A. L. Palma, L. Cina, F. Matteocci, E. Calabrò, A. Di Carlo and T. M. Brown, *Nano Res.*, 2018, **11**, 2669–2681.

S14 M. Li, C. Zhao, Z. K. Wang, C. C. Zhang, H. K. H. Lee, A. Pockett, J. Barbé, W. C. Tsoi, Y. G. Yang, M. J. Carnie, X. Y. Gao, W. X. Yang, J. R. Durrant, L. S. Liao and S. M. Jain, *Adv. Energy Mater.*, 2018, **8**, 1801509.

S15 R. Cheng, C. C. Chung, H. Zhang, F. Liu, W. T. Wang, Z. Zhou, S. Wang, A. B. Djurišić and S. P. Feng, *Adv. Energy Mater.*, 2019, **9**, 1901980.

S16 H. D. Pham, S. M. Jain, M. Li, Z. K. Wang, S. Manzhos, K. Feron, S. Pitchaimuthu, Z. Liu, N. Motta, J. R. Durrant and P. Sonar, *Adv. Electron Mater.*, 2020, **6**, 1900884.

S17 F. Zhang, Z. Yao, Y. Guo, Y. Li, J. Bergstrand, C. J. Brett, B. Cai, A. Hajian, Y. Guo, X. Yang, J. M. Gardner, J. Widengren, S. V. Roth, L. Kloo and L. Sun, *J. Am. Chem. Soc.,* 2020, **141**, 19700–19707.

S18 G. You, Q. Zhuang, L. Wang, X. Lin, D. Zou, Z. Lin, H. Zhen, W. Zhuang and Q. Ling, *Adv. Energy Mater.,* 2020, **10**, 1903146.

S19 Q. Fu, Z. Xu, X. Tang, T. Liu, X. Dong, X. Zhang, N. Zheng, Z. Xie and Y. Liu, *ACS Energy Lett.,* 2021, **6**, 1521–1532.

S20 Y. Hou, X. Y. Du, S. Scheiner, D. P. McMeekin, Z. P. Wang, N. Li, M. S. Killian, H. W. Chen, M. Richter, I. Levchuk, N. Schrenker, E. Spiecker, T. Stubhan, N. A. Luechinger, A. Hirsch, P. Schmuki, H. P. Steinruck, R. H. Fink, M. Halik, H. J. Snaith and C. J. A. Brabec, *Science,* 2017, **358**, 1192–1197.

S21 E. H. Jung, N. J. Jeon, E. Y. Park, C. S. Moon, T. J. Shin, T. Y. Yang, J. H. Noh and J. Seo, *Nature,* 2019, **567**, 511–515.

S22 M. J. Jeong, K. M. Yeom, S. J. Kim, E. H. Jung and J. H. Noh, *Energy Environ. Sci.,* 2021, 2419–2428.

S23 G. W. Kim, J. Lee, G. Kang, T. Kim and T. Park, *Adv. Energy Mater.,* 2018, **8**, 1701935.

S24 J. Lee, G. W. Kim, M. Kim, S. A. Park and T. Park, *Adv. Energy Mater.,* 2020, **10**, 1902662.

S25 L. Zhang, C. Liu, X. Wang, Y. Tian, A. K. Y. Jen and B. Xu, *Adv. Funct. Mater.,* 2019, **29**, 1904856.

S26 J. W. Jo, M.-S. Seo, M. Park, J.-Y. Kim, J. S. Park, I. K. Han, H. Ahn, J. W. Jung, B.Sohn, M. J. Ko. and H. J. Son, *Adv. Funct. Mater.,* 2016, **26**, 4464–4471.